Research on Engineering Structures & Materials

www.jresm.org

Research Group

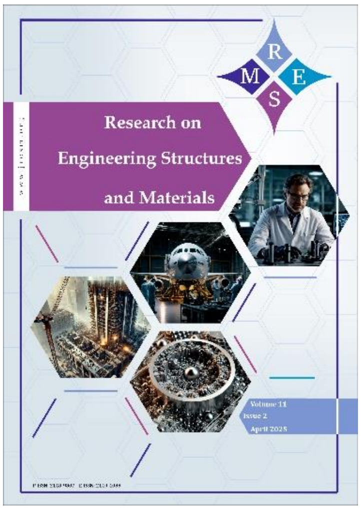

Properties of sustainable concrete incorporating cold-bonded lightweight aggregate manufactured from expired cement, biopolymer, and various waste

Ghazwan F. Khudhair, Waleed A. Abbas

Online Publication Date: 20 June 2025

URL: http://www.jresm.org/archive/resm2025-790ma0327rs.html
DOI: http://dx.doi.org/10.17515/resm2025-790ma0327rs

Journal Abbreviation: *Res. Eng. Struct. Mater.*

To cite this article
Khudhair G F, Abbas W A. Properties of sustainable concrete incorporating cold-bonded lightweight aggregate manufactured from expired cement, biopolymer, and various waste. *Res. Eng. Struct. Mater.*, 2025; 11(6): 2999-3018.

Research on Engineering Structures & Materials
www.jresm.org
Research Group

Research Article

Properties of sustainable concrete incorporating cold-bonded lightweight aggregate manufactured from expired cement, biopolymer, and various waste

Ghazwan F. Khudhair [*,a] , Waleed A. Abbas [b]

Civil Engineering Department, University of Technology, Iraq

Article Info

Article History:

Received 27 Mar 2025

Accepted 16 June 2025

Keywords:

Sustainable concrete; Cold-bonded lightweight aggregate; Expired cement; Waste; Compressive strength; Splitting; Flexural

Abstract

This investigation aims to evaluate the performance of sustainable concrete incorporating artificial coarse aggregate in both its fresh and hard states. The dry reference aggregate mixture, containing 90% fly ash and 10% expired cement, was pelletized utilizing cold-bonded technology. Nine distinct types of aggregates were produced alongside a reference aggregate and subsequently categorized into three groups according to the curing method after a duration of 28 days. This was achieved using the same technique and a water quantity of 20–22% by weight after adding 0.5%, 0.75%, and 1% by weight for each starch, alginate, and tire waste. The reference aggregate categories containing 1% starch (RSS1, ROS1) and 0.75% tire waste (RWR0.75), subjected to self-curing, oven curing, and water curing, represent the optimal formulations of cold-bonded aggregates identified through physical and mechanical testing. Six varieties of sustainable concrete were made by increasing the amount of synthetic coarse aggregate used from 50% to 100%. The water-to-cement ratio stayed at 0.4, and the cement content was kept at 400 kg/m^3. When 50% and 100% of the ROS1 class aggregate were replaced, the density of fresh and hard concrete dropped to its lowest levels, with rates of 7.95%, 16.27%, 10.69%, and 17.63%, respectively. ROS1 aggregate concrete presents exceptional performance across sustainable concrete classifications regarding mechanical characteristics, including compressive strength, splitting, flexural strength, and modulus of elasticity at a 100% replacement rate and an age of 28 days, with decreases of 28.47%, 27.42%, 18.11%, and 36.65% relative to ordinary concrete. Although a good assessment of sustainable concrete styles is according to water absorption test values, normal concrete continues to yield superior outcomes.

1. Introduction

Concrete is the most extensively employed material in the global building industry [1, 2]. The primary constituents of concrete are cement, natural sand, coarse aggregate, and water. It is essential to acknowledge that aggregates, such as sand and gravel, constitute a significant amount, around 70–80%, of the overall volume of concrete [3]. The substantial demand for large amounts of aggregates not only exhausts limited natural resources but also creates considerable environmental sustainability issues [4]. Consequently, there is an immediate necessity to discover alternate choices to either substitute or reduce the use of these aggregates [5]. Moreover, cement that is unused or incorrectly stored will expire if not utilized during the advised storage period and could be classified as waste material [6, 7]. While the production of one ton of cement generates approximately 900 kg of carbon dioxide, which accounts for roughly 5-7% of global CO_2 emissions [8]. As a result, the construction sector has had considerable hurdles for a long time in developing sustainable and environmentally acceptable structures. The density of conventional concrete

*Corresponding author: bce.22.35@grad.uotechnology.edu.iq
[a]orcid.org/0009-0009-1464-0432; [b]orcid.org/0000-0001-8287-2782
DOI: http://dx.doi.org/10.17515/resm2025-790ma0327rs

ranges from 2200 to 2600 kg/m^3 [9]. Lightweight concrete (LWC) often possesses densities ranging from 1400 to 1900 kg/m^3, attributable to the presence of Pores in the lightweight aggregate (LWA). It is characterized by an enhanced strength-to-weight ratio, an appropriate coefficient of thermal expansion, superior strain capacity, and exceptional insulating properties. The implementation of LWC can yield substantial cost reductions by decreasing the dead load of the structure and minimizing the cross-sectional area of steel-reinforced columns, slabs, beams, and foundations [10–12].

Artificial aggregates are typically produced using two methods: cement-based granulation (cold-bonding) and high-temperature burning (sintering)[13, 14]. A significant disadvantage of the sintering process is its elevated energy consumption during granulation. This technique involves the formation of pellets at temperatures up to 1200 °C [15, 16], while the manufacture of aggregates in restricted quantities and high density constitutes a primary obstacle to the extensive industrial implementation of cold bonding technology [5, 13]. In the cold-bonding method, by-products like fly ash, and waste material transform into a water-resistant substance with initially low compressive strength, which increases based on the curing technique and duration [17]. Cold-bonded aggregate offers a viable approach for the advancement of sustainably sourced aggregate manufacturing, providing a solution that conserves valuable natural resources besides transforming waste materials into profitable, environmentally beneficial products [18, 19]. This technique takes into account production parameters including rotation speed, pelletizer angle, pillarization period, and moisture content [20]. Manikandan and Ramamurthy [21] found that low angles and velocities restrict aggregate granule collisions, resulting in a diminutive, ineffective aggregate. Numerous researches have investigated the impact of binder types on lightweight aggregate cold bonding. Gomathi and Sivakumar [22] conducted a comparison of lime- and cement-bound fly ash aggregates. Cement aggregates exhibited a 37% superior crushing strength, a 34% increased dry bulk density, and a 50% reduced water absorption compared to lime aggregates. Studies [23] and [24] show that adding new elements to the reference mix for fly ash aggregate can change its characteristics and enhance some of its attributes. The aggregate particles are influenced by the curing methods employed, analogous to their impact on concrete [15, 25, 26]. The inclusion of cold bonding aggregate (CBA) has been shown to influence the fresh density of concrete, which is associated with the densities of its components. Tang and Brouwers [27] discovered that replacing normal aggregate NA with CBA at change levels of 30% and 60% by volume results in a reduction of fresh density of NAC by approximately 5% and 8%, respectively, while the fresh density of CBAC was identified to be 17% lower than that of NAC [28]. Gesoglu et al. [29] noted that the compressive strength of concrete diminishes when the volume proportion of fabricated cold-bonded fly ash aggregate increases. Joseph with Ramamurthy [30] indicated that synthetic lightweight cold-bonded fly ash aggregate is effective in producing concrete with strengths reaching 52 MPa. The replacement of lightweight fly ash aggregates for normal weight aggregates in concrete led to decreased mechanical characteristics. The study via Kockal and Ozturan [17] indicates that utilizing fly ash aggregate as a complete replacement for normal weight coarse aggregate resulted in a notable reduction in compressive strength and splitting tensile strength, decreasing from 62.9 MPa and 5.1 MPa to 42.3 MPa and 3.7 MPa, correspondingly. Gesoğlu et al. [31] reported analogous findings, demonstrating that the compressive strength and splitting tensile strength of fly ash aggregate concrete diminished from 40.1 and 3.22 MPa to 29.1 and 2.58 MPa, respectively, as the percentage of cold-bonded FA aggregate in concrete with a water-to-cement proportion of 0.35 rose from 30% to 60% of the total aggregate volume in the mixture. Tires provide environmental hazards due to their composition, rendering them highly durable, non-biodegradable, a fire risk, and a breeding ground for rodents and vermin [32]. Hence, much prior research has concentrated on incorporating tire waste into concrete to address several environmental problems related to the accumulation of this waste [33–37]. This study introduces a fresh approach for eco-friendly building systems by producing and assessing the characteristics of sustainable concrete that incorporates replacement ratios of 50-100% of natural coarse aggregate with optimum artificial coarse aggregate created through the cold bonding technique, utilizing a reference mix made from waste materials, including expired cement and used tires.

2. Experimental Program

The practical aspect of this research consists of two parts. The initial stage involved the manufacture of ten types of semi-lightweight coarse aggregates using the cold bonded technique. In the second stage, normal-weight concrete and six varieties of semi-lightweight sustainable concrete were produced by replacing different amounts of natural coarse aggregates with the optimal kind of artificial coarse aggregates.

2.1 Materials

2.1.1 Portland Cement (PC), Expired Cement (EC), Fly Ash (FA)

Portland Cement type CEMI 42.5R, compliant with BS EN 197-1-2011 [38], was employed in the production of normal and sustainable concrete. The expired cement (EC) utilized as a binding agent in the manufacture of coarse aggregate was sourced from cement bags that had been held in the laboratory for almost three months over the expiration date under improper storage circumstances. As shown in Figure 1a, a part of the cement powder has transformed into a semi-solid clumping product and requires re-crushing.

(a)

(b)

Fig. 1. Materials (a) expired cement, (b) fly ash

The Portland cement comprises four primary mineral phases: C3S, C2S, C3A, and C4AF, each possessing distinct properties and specific formation temperatures [39]. The percentage of the four minerals may be computed using the values from table 1 and the Bogue's equations [40] , table 2 presents the conclusive findings about the mass loss proportion between normal cement and expired cement [41, 42]. In the reference mix for artificial aggregate, EC was combined with type F fly ash (Figure 1b) meeting ASTM C618 [43] from EUROBUILD company. Table 1 presents the Properties of PC, EC, and FA.

Table 1. Properties for OPC, EC, FA

Ingredients (%)	Normal Cement OPC	Expired cement EC	Fly ash FA
CaO	62.55	59.92	5.1
Al_2O_3	5.3	4.43	27.7
Fe_2O_3	4.02	3.52	8.44
SiO_2	20.23	20.05	49.66
SO_3	2.27	2.1	0.34
Na_2O	0.21	0.33	0.38
MgO	2.83	2.63	2.65
K_2O	0.91	0.99	3.36
Specific gravity	3.14	3.14	2.1
Loss on ignition	1.01	2.17	3.7

Table 2. Main components of PC, EC

Mass Ratio %	C_3S	C_2S	C_3A	C_4AF
PC	52.98	18.31	7.25	12.22
EC	50.7	19.51	5.79	10.6

2.1.2 Natural Aggregate

Natural sand from the second zone was utilized as fine natural aggregate with a maximum size of 4.75 mm, while crushed gravel functioned as conventional coarse aggregate. Table 2 presents the gradation and characteristics of each kind.

Table 3. Sieve analysis and features of natural aggregates

Fine Aggregate		
Size of Sieve (mm)	Accumulative passing %	Limitations of ASTM C 33[44]
4.75	98	95-100
2.36	92	80-100
1.18	84	50-85
0.6	43	25-60
0.3	23	12-40
0.15	4	0-10
Fineness Modulus	2.56	---
Specific Gravity	2.64	---
Absorption %	2.94	---
Coarse Aggregate		
Size of Sieve (mm)	Accumulative passing %	Limitations of ASTM C 33[44]
19	100	100
12.5	97	90-100
10	65	40-70
4.75	8	0-15
2.36	3	0-5
1.18	1	---
0.6	0	---
0.3	0	---
Fineness Modulus	5.26	---
Specific Gravity	2.68	---
Absorption %	0.61	---
Density (kg/m^3)	1678	---

2.1.3 Tire Waste (R), Starch (S), Alginate (A)

To obtain different types of artificial coarse aggregates, three weight percentages (0.5%, 0.75%, and 1%) of tire waste, starch, and alginate were separately added to the reference mixture. Tire waste granules were collected from the Diwaniyah Tire Factory, with sizes ranging from 0.3 to 0.85 mm. Given the presence of carbon in the microstructure of tire waste granules, which is a soft material impacting aggregate strength, these waste materials were exclusively analyzed using X-ray diffraction (XRD) to more precisely evaluate the effect of tire waste aggregates on the properties of semi-lightweight sustainable concrete. Figure 2 displays test findings revealing carbon levels of up to 75%, oxygen levels of around 17%, and other components ranging from 0.2% to 3%. In this study, both starch and alginate serve as natural biopolymer admixtures. Starch was sourced from local shops, while normal-setting alginate, which dental applications employ as an irreversible hydrocolloid impression substance, demonstrates elastic qualities, obtained from Zhermack Tropicalgin. The widespread consumption of irreversible hydrocolloid surpasses that of any other impression substance [45]. Table 4 presents the chemical characteristics of the substances, whereas. Table 5 delineates their physical characteristics.

Table 4. Chemical characteristics

Chemical Elements	Concentration (ppm)		Percentages
	Starch (S)	Alginate(A)	Tire waste (R)
Iron (Fe)	9.5	---	0.4
Manganese (Mn)	9.6	---	---
Chromium (Cr)	8.4	---	---
Phosphor (P)	45.2	63	---
Sulfur (S)	< 2	906	2.0
Chlorine (CI)	0.3	---	---
Sodium (Na)	< 640	<2100	---
Magnesium (Mg)	< 100	<350	0.2
Aluminum (Al)	< 18	<84	0.6
Silicon (Si)	55.4	17597	0.6
Titanium (Ti)	< 1.5	2431	---
Vanadium (V)	9.5	23.2	---
Calcium (Ca)	45.7	26482	0.4
Potassium (K)	86	---	---
Zink (Zn)	---	---	2.8
Oxygen (O)	---	---	17.2
Carbon (C)	---	---	75.8

Table 5. Physical characteristics

Characteristics	Particle size	Appearance	Density (kg/m^3)	Color
Starch	85.82 nm	Fin Powder	1498	White
Alginate	117.74 nm	Fin Powder	1412	Orang
Tire waste	0.3-0.85 mm	Powder	586	Black

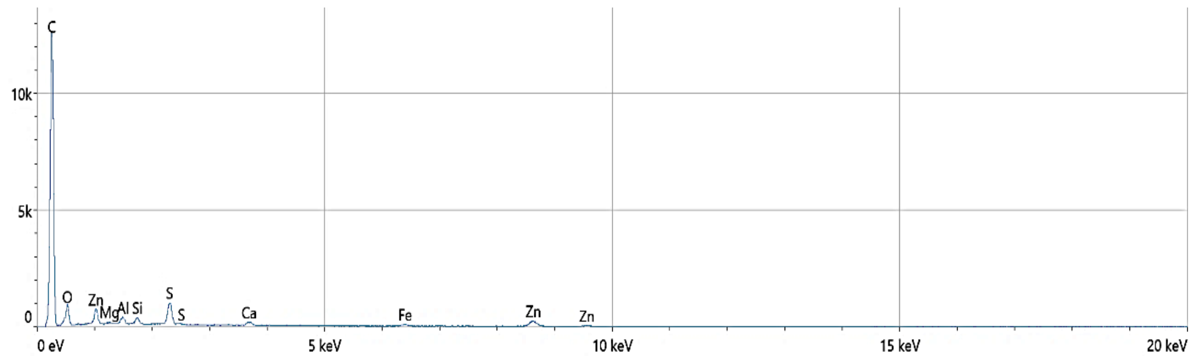

Fig. 2. XRD image for tire waste elements

(a) (b) (c)

Fig, 3. Materials (a) Tire waste, 8b) Starch, (c) Alginate

2.1.4 Superplasticizer

Sika's ViscoCrete-5930 superplasticizer have been choosing for enhancing the workability of concrete and achieve the desired consistency. A third-generation superplasticizer for concrete and mortar, according to the standards for superplasticizers delineated in ASTM C-494 Classes G and F [46], plus BS EN 934 Part 2: 2001[47]. Table 6 offers the characteristics of the superplasticizer [48].

Table 6. Properties of superplasticizer*

Properties	Result [48] *
Dosage	0.8-2 % by weight of cement
Density	1.095 kg/ litter (ASTM C 494) [46]
Storage	5-35° C
Toxicity	Non-toxic
packaging	5-20-200 kg
Appearance	Turbid liquid
Life	12 months from production

* Data from Production Company

2.2 Production of Cold-Bonded Fly Ash Coarse Aggregate

The practical part of this research starts with the creation of synthetic semi-lightweight coarse aggregate at room temperature. This is done using a pelletizing machine and a cold bonding technique for the dry mixture components. The pelletizing apparatus comprises a drum with a depth of 350 mm, a diameter of 850 mm, an operating angle of 90 degrees, and a rotational speed of up to 45 rpm like seen in the figure 4. Through previous investigations [23, 25, 49, 50] and several trials, the optimal operational parameters of the machine were established, including speed, inclination angle, and water amount. The dry reference mixture, including 90% fly ash and 10% expired cement, is poured in the container and blended at a rotational speed of 4 to 6 rpm to attain homogeneity. The device's water pumps release water in three successive batches, maintaining a water-to-mixture ratio of 20% to 22% by weight. After the initial 10 minutes, freshly spherical pellets start formation.

Table 7. Sieve analysis of lightweight coarse aggregate (LWCA)

Sieve size (mm)	LWCA	%Passing - ASTM C330
19	100	100
12.5	96	90-100
9.5	57	40-80
4.75	10	0-20
2.36	2	0-10

The agglomeration process extends for an extra 10 minutes to guarantee the grains attain the requisite size and enough hardness for handling. Upon completion of the pelletizing process, the resultant aggregate is held in sealed plastic bags for 24 hours at a temperature of 20 degrees Celsius, with a permissible variation of ±2 degrees, and a humidity level of 70% [51]. Executed three separate curing methods on 10 aggregate classes during a 28-day period: self-curing, water-curing, and oven-curing at a temperature of 64°C. Oven curing elevates the specific gravity and bulk density of lightweight coarse aggregate from 1.85 and 976 kg/m^3 for water-cured aggregate and from 1.87 and 984 kg/m^3 for self-cured aggregate to 1.92 and 1012 kg/m^3, respectively. The heat-curing regimes result in enhanced hydration dynamics, which provide a denser structure [52], while the LWCA pellets disintegrate owing to water curing [49]. Furthermore, oven curing achieved the maximum crushing strength values of the aggregate at 9.24 MPa, reflecting an increase of 0.32% relative to the self-cured aggregate and 5.84% compared to the water-cured aggregate. Subsequently, a sieve analysis was performed in accordance with ASTM C330 [53]. According to the criteria stated in BS-812-110-1990[54], the crushing strength of the particle for ALWA was assessed using the California Bearing Ratio (CBR). Employing ASTM C127[55] to ascertain the specific gravity of the lightweight aggregate in a saturated surface dry condition and its water absorption capacity.

(a) (b) (c) (d)

Fig. 4. Steps for manufacturing artificial coarse aggregate via the cold bonding technique (a) Pelletizer disc, (b) Dry powder, (c) Homogeneity of ingredients, (d) Formation of pellets

2.2.1 Scanning Electron Microscopy Test (SEM)

Figures 5 a, b, and c present S.E.M. analysis of aggregate particles roughly 1 cm in size for the optimum categories of the produced aggregate (RSS1, ROS1, RWR0.75). Photographs taken with a scanning electron microscope show the interior structure and illustrate the development of various pore patterns. The primary distinction among ideal aggregation types is in the pores, which may be circular, unconnected, and irregular, or linked and longitudinal. The oven-cured granules demonstrate enhanced homogeneity in their exterior matrix and a more robust structure due to improvements in the hydration dynamics, in contrast to the water-treated granules, which experienced degradation in their external matrix and an enlargement of pore size. The self-cured aggregate particles exhibit a surface and microscopic structure of moderate solidity. Microstructure investigations suggest that a closed structure formed from the interaction between the components of the additional substance and calcium hydroxide (portlandite) in the reference mix may account for the diminished water absorption ratio of the optimal lightweight aggregates ROS1.

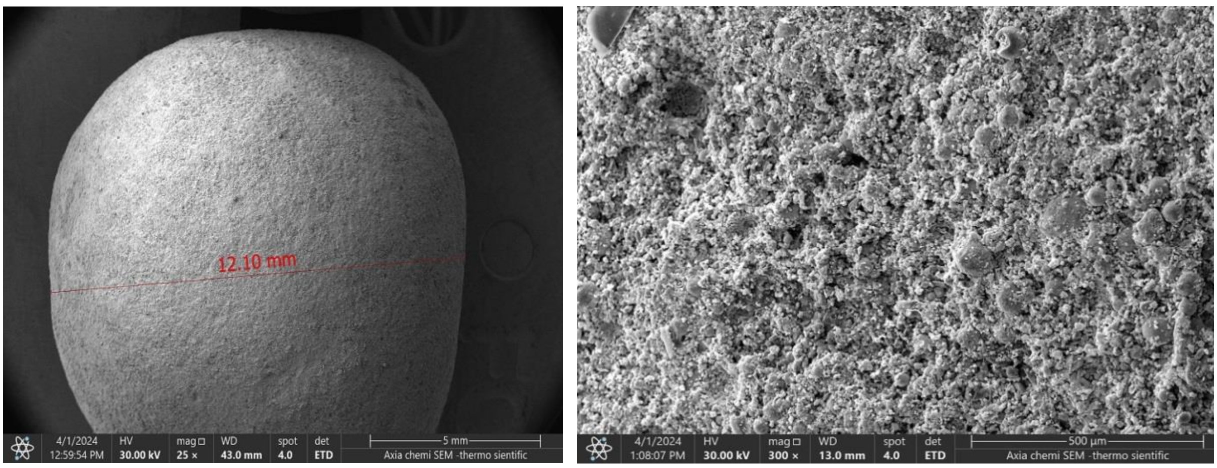

(a)

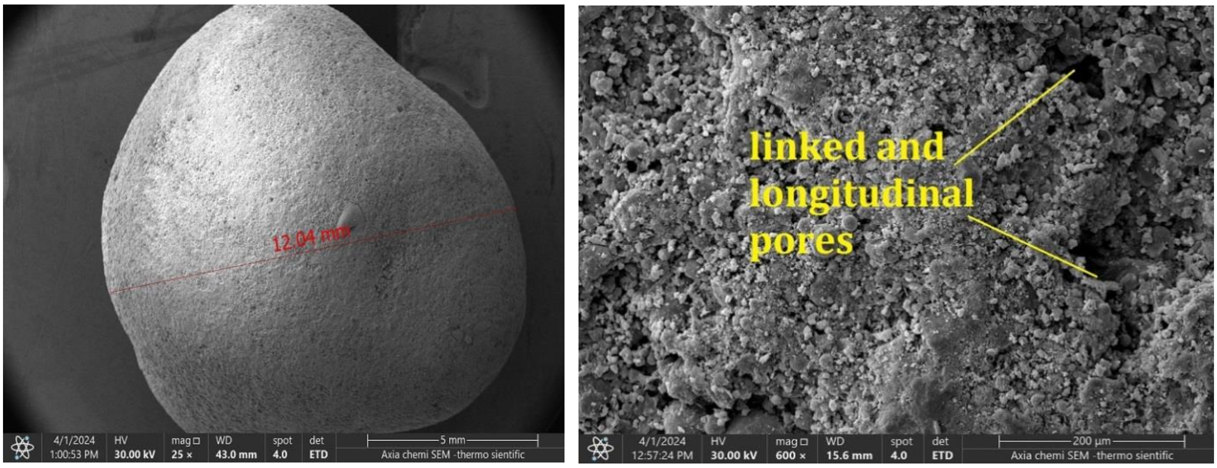

(b)

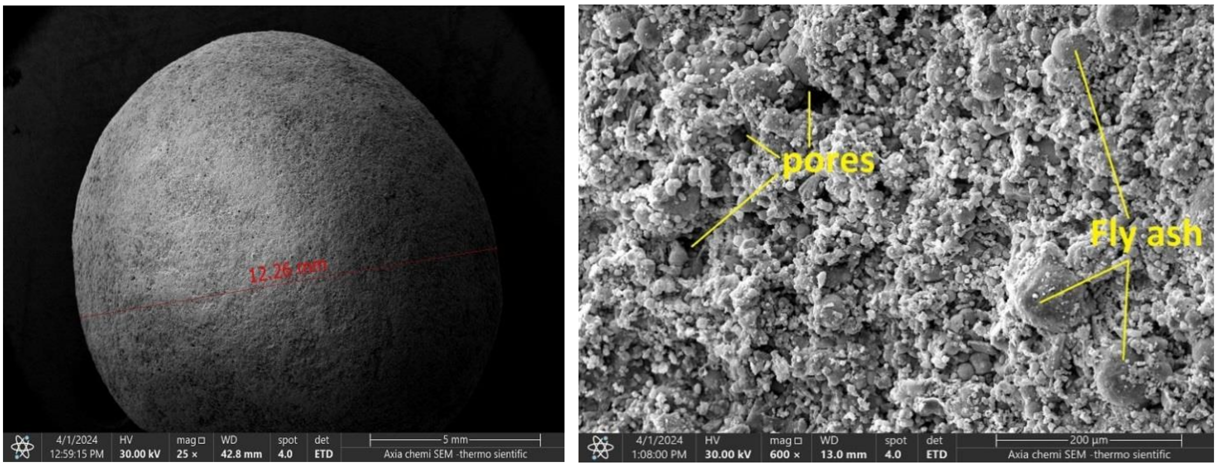

(c)

Fig. 5. SEM analysis (a) Oven-Cured Aggregate with 1% Starch (ROS1), (b) Water-Cured Aggregate with 0.75% Tire waste (RWR0.75) and (c) Self-Cured Aggregate with 1% Starch (RSS1)

3. Mix Proportions of Concrete

This section covers the experimental program's strategy for creating semi-lightweight sustainable concrete using the best types of coarse aggregates (RWR0.75, RSS1, ROS1) that the study's initial phase produced and identified. To assess the influence of this aggregate type, a reference concrete was formulated containing 100% natural aggregate (NA), 400 kg /m^3 cement quantity, and a ratio of water to cement W/C 0.4. Additionally, a sustainable concrete was made by substituting the natural coarse aggregate (NCA) with synthetic lightweight coarse aggregate (LWCA) at volumetric proportions of 50% and 100%, respectively, while maintaining the weights of the other components of the concrete mix constant. To achieve a 120 mm slump in conventional concrete and a 75 mm slump in sustainable concrete while ensuring modified workability, the dose of superplasticizer was tailored for each concrete mix [56]. The adjustment is primarily due to the spherical morphology of lightweight coarse aggregate (LWCA), in contrast to the angular characteristics of normal coarse aggregate (NCA), which required an extra superplasticizer dose [57–59]. This work employed an electric rotary mixer with a capacity of 1 cubic meter, as depicted in figure 6. Artificial coarse aggregate particles must reach a state of saturation and a dry surface (SSD) before manufacturing, as their ability to absorb significant amounts of water negatively affects the concrete [41, 60]. Consequently, the weights of the aggregates utilized in the generated mixtures were altered according to the absorption rate of each type, attaining the saturated surface dry (SSD) condition [40]. The document ACI 211.2-98 [61] outlines protocols for formulating concrete mixes. The ratio of concrete components for one cubic meter is presented in table 8.

Table 8. Details mix proportions for concrete kg/m^3

Mixes designation*	Cement kg/m^3	NFA kg/m^3	NCA kg/m^3	LWCA kg/m^3	W/C ratio	Super plasticizers%	Slump mm
NWC	400	656	1024	0	0.4	1.3	120
50RSS1C	400	656	512	350.88	0.4	1.005	75
100RSS1C	400	656	0	701.76	0.4	0.946	75
50RWR0.75C	400	656	512	357.12	0.4	1.107	75
100RWR0.75C	400	656	0	714.24	0.4	0.964	75
50ROS1C	400	656	512	362.17	0.4	0.982	75
100ROS1C	400	656	0	724.34	0.4	0.642	75

*Note: W/C : water-to-cement ratio; NWC : normal weight concrete; NFA : natural fine aggregate; NCA : natural coarse aggregate; LWCA : lightweight coarse aggregate; RSS1 : self-cured aggregate with 1% starch; ROS1 : oven-cured aggregate with 1% starch; RWR0.75 : water-cured aggregate with 0.75% tire waste; RSS1C, ROS1C, and RWR0.75C represent sustainable concrete incorporating 50% and 100% lightweight coarse aggregate.

(a) (b)

(c) (d)

Fig. 6. Concrete production process (a) Artificial aggregate immersed in water, 8b) Electric blender 1m^3, 8c) Slump checking, (d) Concrete pouring

4. Methodology for Sample Preparation and Testing

Conforming with BS EN 12390-3 [62] determined the compressive strength using a 100 x 100 x 100 mm test cube. The test was performed on three specimens at 7, 28, and 60 days of age, employing a 2000 KN compression apparatus with a loading rate of 15 N/mm per minute, Prior to that, Ultrasonic Pulse Velocity of these samples are examined in line with ASTM C597 [63]. The mean of three results for each test age is extracted through inputting the readings of each sample into Equations 1 and 2.

$$f_{cu} = \frac{P}{A} \tag{1}$$

where, f_{cu}: The compressive strength MPa, P: Load failure (N), A: Cross-section area (mm^2).

$$\mathcal{V} = \frac{L}{T} \tag{2}$$

where, V: Ultrasonic pulse speed meter/second, L: path length (m), T: pulse transit period (sec).

As per ASTM C642-13 [64], this study checks the density of concrete and the absorption ratio at different curing ages by heating samples in an oven at 110 ± 5 degrees Celsius for 24 hours. Once the specimens reached room temperature, recorded their weight (A). Later returned them to the water tanks. Following an additional 24 hours, documented the samples' weight in water (C) and allow them to air dry at room temperature until they reach a saturated and surface-dry condition, after which measured their weight (B). The splitting tensile strength was calculated on three cylindrical samples, each measuring 100 × 200 mm, in line to the specified testing age [65]. Slender plywood bearing strips are employed to evenly distribute the tension exerted across the cylinder's length when put inside the test machine. Equation 3 is applied to ascertain the outcomes figure 7.

$$f_t = \frac{2p}{\pi L d} \tag{3}$$

where, f_t: splitting tensile strength MPa, P: Maximum apple load (N), L: Length of specimen (mm), d: Diameter of specimen (mm).

Prism-shaped models measuring 100 mm by 100 mm by 400 mm are utilized to examine flexural strength corresponding with ASTM C78[66] the formula 4 serves to determine the values that can symbolize the rupture modulus. Figure 7 depicts the sample and the device used.

$$f_r = \frac{p \times l}{b \times d^2} \tag{4}$$

where, f_r: flexural strength MPa, p: Maximum load (N), L, b, d: Length, Width, Depth, of specimen.

The final findings of the Static Modulus of Elasticity test reflect the average values obtained from three cylinders measuring 100 by 300 mm at ages of 28 and 60 days, which meet with ASTM C469 [67]. The equation 5 was utilized to ascertain the ratio of stress to strain and the ratio of longitudinal strain to lateral strain of hardened concrete under specified curing conditions.

$$E_c = \frac{S_2 - S_1}{\varepsilon_2 - 0.00005} \times 10^{-3} \tag{5}$$

where, E_c: Elastic modulus GPa, S_1: Stress correlated with longitudinal strain of 0.000050 MPa, S_2: Stress equivalent to 40% of the ultimate load MPa, ε_2: Longitudinal strain induced by stress S2.

(a) (b) (c) (d)

Fig. 7. Concrete specimens and examination devices: (a) Oven, (b) Splitting, (c) Flexural, (d) Modules of elasticity

5. Findings and Discussion

5.1 Density

Table 9 illustrates the disparity in fresh density results between conventional concrete and sustainable concrete, with the latter's density consistently diminishing as the ratio of natural coarse aggregate replaced by artificial lightweight coarse aggregate increases, owing to the porous characteristics of the lightweight aggregate particles [68]. The density values vary from 2427 kg/m^3 to 2032 kg/m^3. These results align with [18, 56, 69], specific gravity, and bulk density of each aggregate type selected. The change in specific gravity of the components in the concrete mixes results in differing dry density values. As illustrated in Figure 8, the values rise as the concrete matures because of ongoing hydration, gel formation, and enhancements in the properties of the interfacial transition zone. Nonetheless, their performance declines when manufactured coarse aggregate exceeds 50% as a substitute for natural coarse aggregate [70].

Table 9. Density mixes of concrete

Mix Designation	weights of Cubes for Concrete Mixtures(kg)	Fresh Concrete Density kg/m^3
NWC	11.26	2427
50RWR0.75	11.09	2254
100RWR0.75	10.91	2078
50RSS1	11.13	2293
100RSS1	10.92	2081
50ROS1	11.07	2234
100ROS1	10.87	2032

Conventional concrete exhibits superior performance due to the elevated specific gravity of the natural coarse aggregate and its low porosity [18]. The densities of concrete incorporating 50% and 100% ROS1 aggregate diminished at the most significant rates (10.99%, 10.69%, 10.78%, and 17.56%, 17.63%, 17.66%), respectively, relative to conventional concrete during the designated testing dates. This was due to a decrease in the overall specific gravity and density of the aggregate particles. Even though RSS1 aggregate concrete's dry density values keep going down compared to normal concrete, it performs better than ROS1 and RWR 0.75 aggregate concrete because the aggregate particles have a higher specific gravity and density. The test results demonstrated that the dry density of the semi-lightweight sustainable concrete corresponds with prior research findings [71].

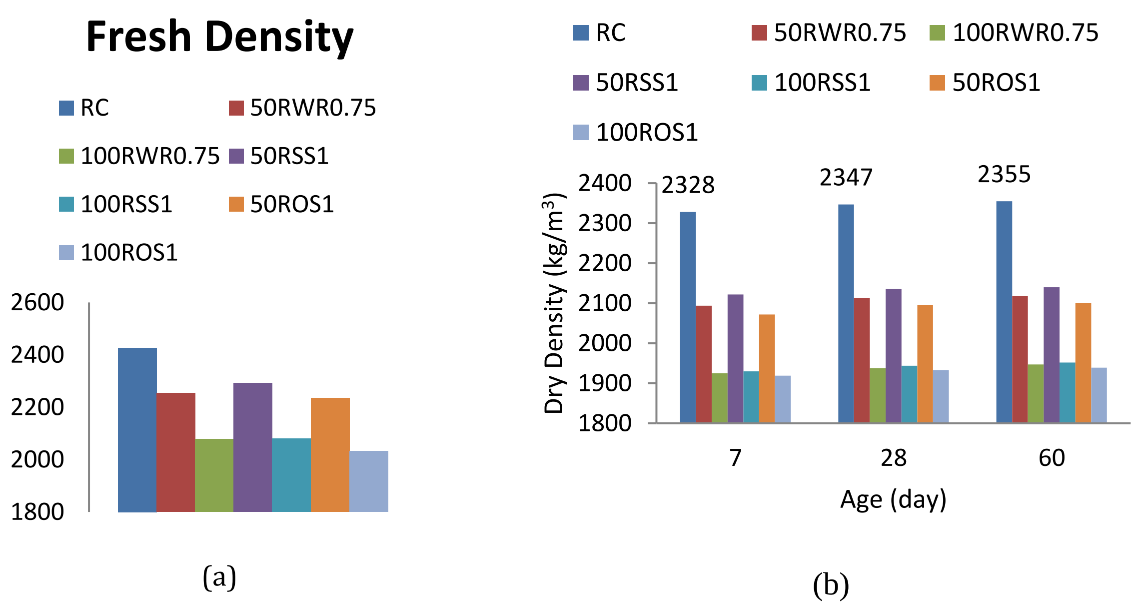

Fig. 8. Density: (a)Fresh density, (b) Dry density

5.2 Ultrasonic Pulse Velocity (UPV)

The results of this test improve as both normal and sustainable concrete mature due to ongoing hydration and the evolution of hydration products that enhance structural integrity. However, the velocity of ultrasonic pulse transmission in the standard concrete model is superior to that in the sustainable concrete, owing to its higher density and more effective filling of pores with hydration products [41, 71]. The test assesses the quality of the concrete, the uniformity of its internal components, and the impact of voids by measuring the pulse propagation velocity between the two sides of the sample. Figure 9 demonstrates a reduction in pulse transmission velocity as the proportion of natural coarse aggregate substituted with lightweight artificial aggregate escalates from 50% to 100%. The drop attains its minimum in concrete containing 100% ROS1 type aggregate 3625, 3628, and 3629 m/s, demonstrating reduction rates of 21.09%, 21.79%, and 25.80% relative to conventional concrete 4594, 4639, and 4891 m/s at 7, 28, and 60 days, respectively, attributable to the low bulk density of ALWA [72]. However, it is still classified as good concrete in accordance with ASTM C597[73]. In contrast, the concrete incorporating 50% RSS1 class aggregate had the highest pulse arrival velocity, 4111, and 4112 reaching a maximum of 4115 meters per second at 60 days, and is classified as excellent concrete. Figure 9 depicts that all concrete mixtures generated in this investigation are classified from good to excellent according to ASTM C 597-02 specifications [73].

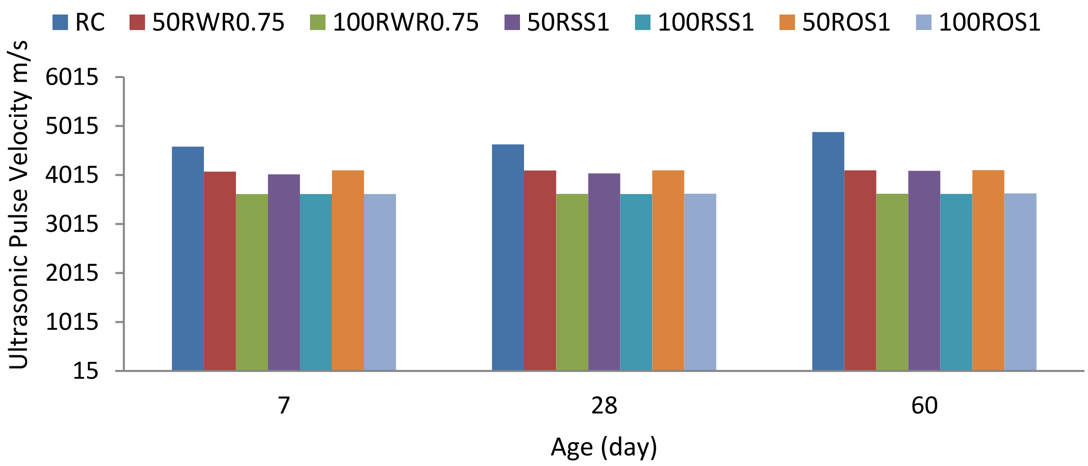

Fig. 9. Ultrasonic Pulse Velocity Results

5.3 Compressive Strength

The compressive strength of concrete indicates its quality and reflects its other characteristics. Figure 10 displays a drop in concrete strength when the ratio of natural coarse aggregate substituted with artificial coarse aggregate rises, due to the disparity in strength between the two aggregate types [71, 74]. Conversely, regardless of the replacement ratios, prolonged water curing improves the strength of the concrete due to the ongoing hydration process. This process results in the formation of additional materials, such as calcium silicate hydrate (C-S-H), which in turn enhances the internal structure's integrity [18, 41]. This investigation used a reference concrete that included natural aggregate, which exhibited compressive strengths of 39.7, 49.35, and 57 MPa at the designated testing ages, and sustainable concrete, with 50% and 100% replacement for ideal cold-bonded lightweight aggregate categories. Evaluations were conducted at 7, 28, and 60 days of curing. The type two concrete results were between 31.5 and 45.7 MPa, which is in line with the ASTM C330 [53] and ACI 318 [75] standards for structural lightweight concrete, which say that the concrete must have a minimum 28-day compressive strength of 17.2 MPa. Employing a 50% and 100% replacement ratio of aggregate class RWR0.75, the strength of semi-lightweight sustainable concrete diminishes to its lowest of 35.4, 38, 40.9 ,31.5, 33.25, and 35 MPa, demonstrating a decline rate of 10.83%, 22.99%, 28.24%, 20.65%, 32.62%, and 38.59% in a 7, 28, and 60-day test, respectively. The reduced solidity of the aggregate particles containing rubber negatively affects the overall strength of the concrete [76]. The concrete aggregate type RSS1 comes with average values of 36.6, 38.45, 41.77, 33.1, 34.14, and 36.28, respectively, as illustrated in figure 10. During this test, concrete made with aggregate ROS1 did better than other sustainable concrete mixes. This is because heat curing processes influence aggregate particles, which leads to the highest crushing strength [25, 52, 71]. The findings align with [56, 77].

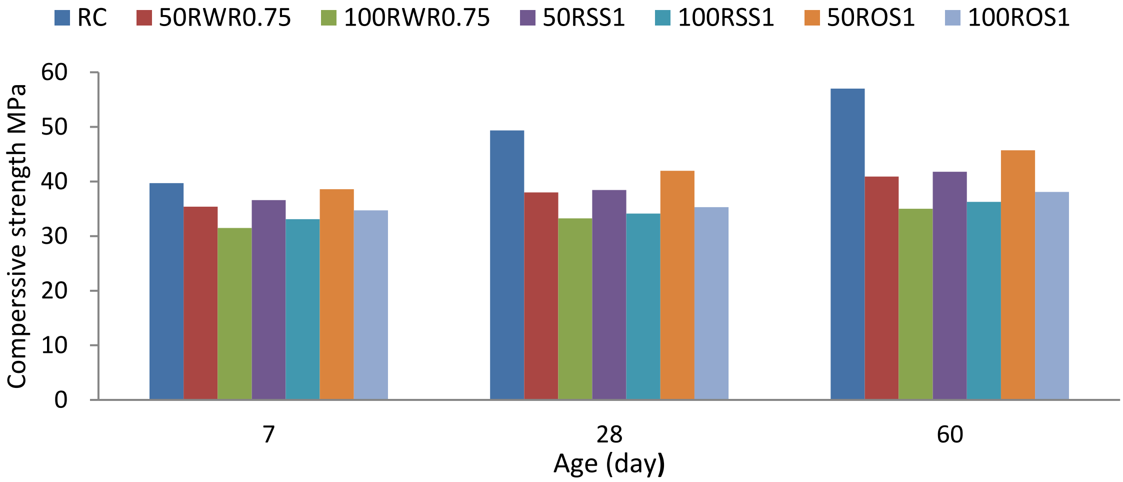

Fig. 10. Compression strength at 7, 28, and 60 day

5.4 Splitting Tensile Strength

The partially or complete substitution of natural coarse aggregate with synthetic lightweight coarse aggregate diminishes the splitting tensile force of concrete at testing ages of 7, 28, and 60 days [68]. This results from the low tensile strength of the ALWA particles and the existence of empty voids in their structure, which cause failure along paths aligned with these pores [18]. Figure 11 display test results that vary from 3.4 to 4.3 MPa for standard concrete and from 1.6 to 4.1 MPa for sustainable concrete. An examination of various semi-lightweight concrete types at 50% and 100% replacement levels indicates that ROS1 aggregate concrete has the highest splitting tensile strength, with lowering rates of 17.64%, 5.71%, and 4.65%, as well as 25.85%, 27.42%, and 38.37%, respectively, in comparison with natural aggregate concrete. On the other hand, concrete involving coarse aggregate type RWR0.75 gives the lowest results at all specified testing dates. This is due to the inherent fragility of the industrial aggregate [78, 79].

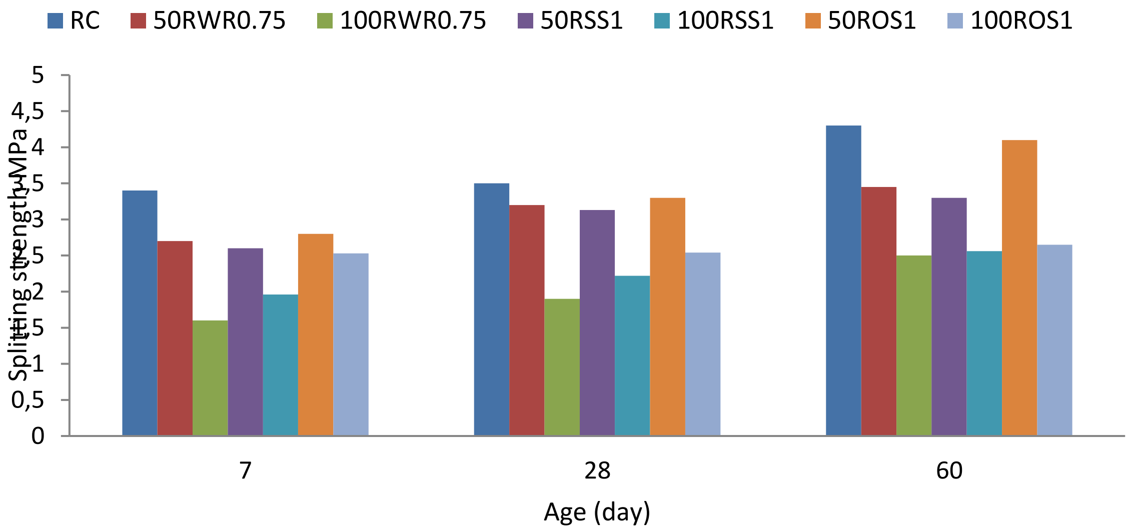

Fig. 11. Splitting tensile strength

5.5 Flexural Strength

This attribute enhances over time in normal and sustainable concrete owing to advancements in the curing and hydration processes [80]. The flexural strength of regular concrete is higher than that of sustainable concrete at all testing ages and replacement ratios, as shown in figure 12. This is mostly because natural coarse aggregate is stronger [20, 68]. Normal concrete had test results ranging from 5.5 to 8.5 MPa, while sustainable concrete had results ranging from 2.92 to 7.92 MPa after the required curing times. Compared to the other types of concrete that used coarse industrial aggregate, ROS1 aggregate concrete did better at 7 and 28 days, reaching a peak 7.92 MPa after 60 days with a 50% replacement, attributable to the strength of the aggregate [18]. As illustrated in figure 12, RSS1 aggregate concrete demonstrates average performance. Conversely, the RWR0.75 aggregate concrete exhibits weaker performance relative to conventional concrete, with decreasing rates (12, 25.76, 27.05) at 50% replacement and 46.9, 62.24, and 60.23 at 100% replacement, owing to the negative effect of rubber on the strength of aggregate grains [76].

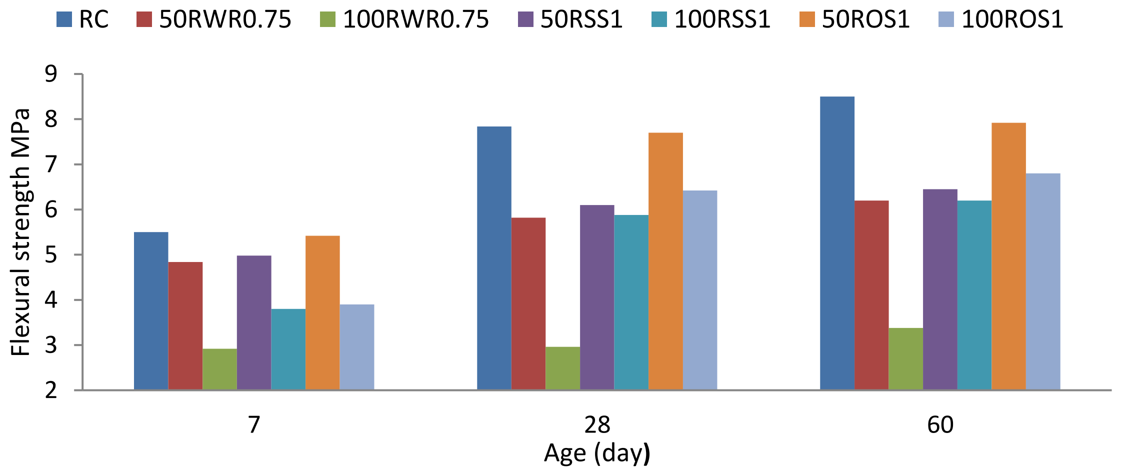

Fig. 12. Flexural strength

5.6 Modulus of Elastic (E_c)

Properties of the aggregate (strength, structural composition, amount used) affect the modulus of elasticity of concrete [29], with these values varying according to changes in concrete compressive strength (goes up or down) [18]. Figure 13 exhibit that the modulus of elasticity values to all category's concrete get stronger over time [68], which ranges from 27.57 GPa at 7 days to 33.54 GPa at 60 days for normal concrete.

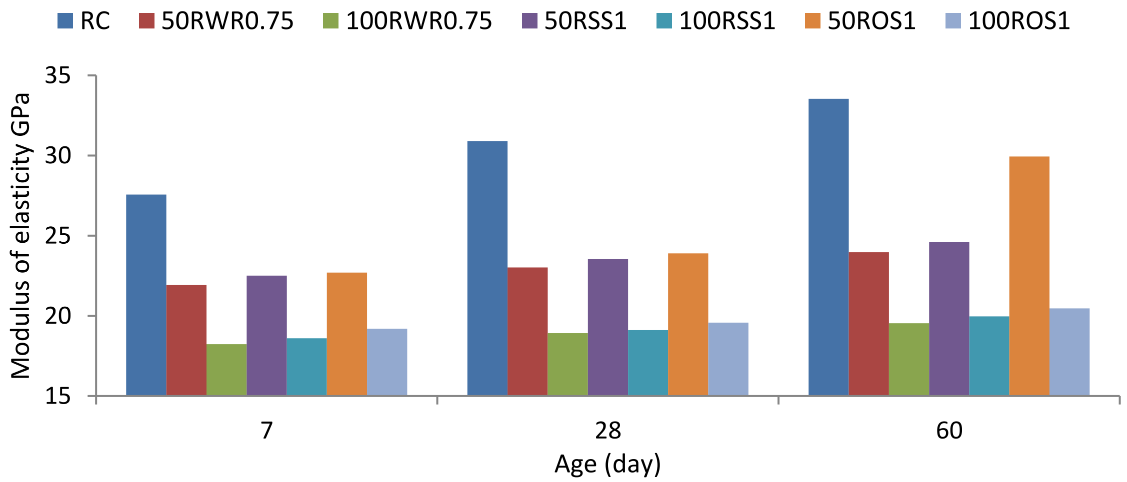

Fig. 13. Modulus of Elastic

In contrast, the modulus of elasticity for sustainable concrete differs from a minimum of 18.23 GPa at 7 days to a maximum of 29.94 GPa after 60 days of curing, attributable to the superior strength and less porous structural composition of natural coarse aggregate compared to artificial coarse lightweight aggregate [81]. Figure 13 demonstrates that the modulus of elasticity declines when the lightweight aggregate (LWA) replacement percentage increases from 50% to 100% [18, 82]. For example, among similar types, concrete employing coarse aggregate of type ROS1 works the best, while the incorporation of 50%, 100% RWR0.75 aggregate results in a decline in the concrete's elastic modulus by 20.49%, 25.52%, 28.53%, and 33.87%, 38.79%, 41.74% after 7, 28, and 60 days, respectively, in comparison to concrete made with natural aggregate. The RSS1 aggregate concrete possesses average values.

5.7 Water Absorption

Porosity significantly affects the properties of concrete regarding water absorption, as it creates channels for water infiltration and movement inside its structural matrix, hence augmenting the amount of absorbed water. Figure 14 demonstrates a decline in these ratios as curing age advances for concrete mixtures, due to the continuous hydration process and the formation of additional calcium silicate gel, which reduces pore size and their connectivity [72], while simultaneously improving the strength of the interfacial transition zone. In standard concrete, water is absorbed mainly by the cement paste; however, in sustainable concrete (semi-lightweight), it is absorbed by both the cement paste and the coarse artificial aggregate due to its porous properties. As a result, sustainable concrete displays a higher absorption of water than conventional concrete [83, 84]. The test values ranged from 4.6 to 3.2 for standard concrete and from 10.24 to 5.22 for sustainable concrete across planning age categories. The concrete with ROS1 type aggregate at a 50% ratio exhibited notable performance at 7 and 28 days, approaching optimal conditions after 60 days with a 38.69% increase relative to conventional concrete, aligned with improvements in aggregate particle characteristics [10]. At the identical replacement percentage, the concrete incorporating RWR0.75% aggregate exhibited an elevation in absorption values, attributable to the heightened absorption of the aggregate assessed in the initial part of the investigation. The elevated water absorption rate of the RSS1 type aggregate led to a corresponding rise in the concrete absorption rate, achieving the maximum values, with increases of 44.24%, 55.34%, and 58.81% relative to standard concrete. The amount of water permeating the concrete is associated with the presence of pores; hence, figure 14 depicts its increase when the substitute ratios of natural coarse aggregate with lightweight artificial coarse aggregate change from 50% to 100%, in accordance with research findings [41, 85]. Except for the test result for the 7-day-old concrete made of 100% RSS1 class aggregate, the sustainable concrete mixes developed in this study are very good, as shown by the fact that they didn't absorb more than 10% [9].

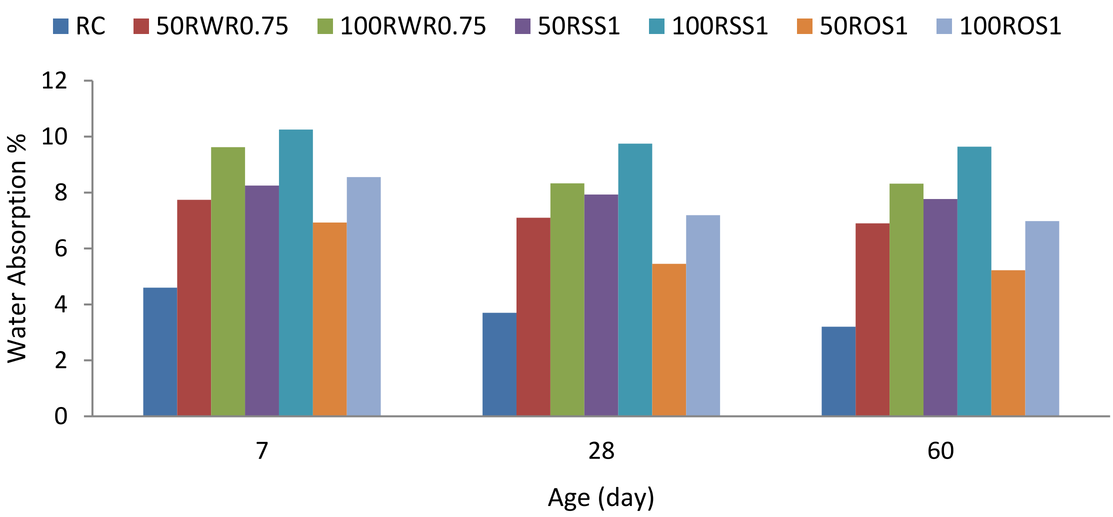

Fig. 14. Water absorption

6. Conclusion

The findings of the experimental program in the present research yield the following conclusions:

- Conventional concrete has superior performance compared to concrete with an equivalent blend of natural and artificial coarse aggregates. The latter performs better than concrete that completely employs synthetic coarse aggregate.
- In the Ultrasonic Pulse Velocity test, normal concrete attained findings categorizing it as excellent, whereas the assessment of sustainable concrete varied from excellent at 50% replacement ratios to good at 100% replacement ratios.
- The compressive strength of concrete generally diminishes while the growing substitution of natural coarse aggregate with artificial coarse aggregate. Owing to the influence of aggregate particle strength on this property, RWR0.75 aggregate concrete exhibits the lowest values among the various types of produced aggregates at 28 days, with reduction rates of 22.99% and 32.62% relative to normal concrete. Concurrently, ROS1 aggregate concrete demonstrates better results, with decline rates of 14.99% and 28.47%, respectively.
- As the fraction of ROS1 aggregate usage increases from 50% to 100%, the rates of fresh density reduction in sustainable concrete rise from 7.95% to 16.27% in comparison to normal concrete. The documented outcomes for this aggregate type are the lowest in comparison to RSS1 and RWR0.75 aggregates.
- Semi-lightweight sustainable concrete that uses manufactured coarse aggregate doesn't need as much superplasticizer as regular concrete that uses natural coarse aggregate. The decrease becomes more evident when the ratio of artificial aggregates used instead of natural aggregates increases.
- Achieving a replacement rate of 100%, ROS1 aggregate effectively diminished the dry density of sustainable concrete, registering the lowest values with a decline rate of 10.69% and 17.66% at 28 and 60 days, respectively.
- The superior quality of the natural aggregate supplied enhances the performance of normal concrete in tests of splitting, flexural, and elasticity. The results of these examinations decline with the use of coarse industrial aggregate, proportional to the quantities employed. This investigation revealed that the sustainable concrete ROS1-type aggregate exhibited positive findings, with reductions of 27.42%, 18.11%, and 36.56%, respectively, after 28 days.
- Despite the reduction in water absorption rate with the aging of concrete, normal concrete maintains lower results compared to sustainable concrete. The absorption rate of the aggregate influences this attribute. The concrete incorporating ROS 1 aggregate at 50% and 100% yields good results, with increases of 32.11% and 48.35%, respectively, at a 28-day testing period.

Reference

[1] Tenza-Abril AJ, Compañ-Rosique P, Satorre-Cuerda R, et al. Smartphone Application for Determining the Segregation Index of Lightweight Aggregate Concrete. Sustainability 2021; 13: 12564. https://doi.org/10.3390/su132212564

[2] Kabay N, Mert M, Miyan N, et al. Pumice as Precursor in Geopolymer Paste and Mortar. J Civ Eng Constr 2021; 10: 225-236. https://doi.org/10.32732/jcec.2021.10.4.225

[3] Almeshal I, Tayeh BA, Alyousef R, et al. Use of recycled plastic as fine aggregate in cementitious composites: A review. Constr Build Mater 2020; 253: 119146. https://doi.org/10.1016/j.conbuildmat.2020.119146

[4] Hamada HM, Alattar AA, Yahaya FM, et al. Mechanical properties of semi-lightweight concrete containing nano-palm oil clinker powder. Phys Chem Earth, Parts A/B/C 2021; 121: 102977. https://doi.org/10.1016/j.pce.2021.102977

[5] Özkan H, Kabay N, Miyan N. Properties of Cold-Bonded and Sintered Aggregate Using Washing Aggregate Sludge and Their Incorporation in Concrete: A Promising Material. Sustain; 14. Epub ahead of print 2022. https://doi.org/10.3390/su14074205

[6] Ibrahim H, Abbas W. Fresh Properties of Self-Consolidating Expired Cement-Fly Ash Cold Bonded Lightweight Aggregate Concrete with Different Mineral Admixtures. Eng Technol J 2023; 41: 734-744. https://doi.org/10.30684/etj.2023.139260.1424

[7] Meddah A, Chikouche MA, Yahia M, et al. The Efficiency of Recycling Expired Cement Waste in Cement Manufacturing: a Sustainable Construction Material. Circ Econ Sustain 2022; 2: 1213-1224. https://doi.org/10.1007/s43615-022-00161-1

[8] Bordy A, Younsi A, Aggoun S, et al. Cement substitution by a recycled cement paste fine: Role of the residual anhydrous clinker. Constr Build Mater 2017; 132: 1-8. https://doi.org/10.1016/j.conbuildmat.2016.11.080

[9] A. M. Neville. Properties of concrete Fifth. 2009.

[10] Abbas ML, Abbas WA. Influence of Novel Cold Bonded Attapulgite Lightweight Aggregate on the Performance Properties of Lightweight Aggregate Concrete. University of Technology, 2023.

[11] Ibrahim MA, Atmaca N, Abdullah AA, et al. Mechanical properties of concrete produced by light cement-based aggregates. Sustainability 2022; 14: 15991. https://doi.org/10.3390/su142315991

[12] Kumar R, Srivastava A, Lakhani R. Industrial wastes-cum-strength enhancing additives incorporated lightweight aggregate concrete (LWAC) for energy efficient building: A comprehensive review. Sustainability 2021; 14: 331. https://doi.org/10.3390/su14010331

[13] Güneyisi E, Gesoğlu M, Pürsünlü Ö, et al. Durability aspect of concretes composed of cold bonded and sintered fly ash lightweight aggregates. Compos Part B Eng 2013; 53: 258-266. https://doi.org/10.1016/j.compositesb.2013.04.070

[14] Cioffi R, Colangelo F, Montagnaro F, et al. Manufacture of artificial aggregate using MSWI bottom ash. Waste Manag 2011; 31: 281-288. https://doi.org/10.1016/j.wasman.2010.05.020

[15] Mohamad Ibrahim N, Ismail KN, Che Amat R, et al. Properties of cold-bonded lightweight artificial aggregate containing bottom ash with different curing regime. E3S Web Conf; 34. Epub ahead of print 2018. https://doi.org/10.1051/e3sconf/20183401038

[16] Rosicki Ł, Narloch P. Studies on the ageing of cement stabilized rammed earth material in different exposure conditions. Materials (Basel) 2022; 15: 1090. https://doi.org/10.3390/ma15031090

[17] Kockal NU, Ozturan T. Effects of lightweight fly ash aggregate properties on the behavior of lightweight concretes. J Hazard Mater 2010; 179: 954-965. https://doi.org/10.1016/j.jhazmat.2010.03.098

[18] Abbas ML, Abbas WA, Güneyisi E. Shrinkage and thermo-mechanical properties of concretes incorporated with different substitutions of natural aggregates by cold bonded calcined attapulgite lightweight aggregates. J Build Eng 2023; 79: 107921. https://doi.org/10.1016/j.jobe.2023.107921

[19] Thomas J, Harilal B. Sustainability evaluation of cold-bonded aggregates made from waste materials. J Clean Prod 2019; 237: 117788. https://doi.org/10.1016/j.jclepro.2019.117788

[20] Ibrahim MA, Atmaca N. Cold bonded and low temperature sintered artificial aggregate production by using waste materials. Period Polytech Civ Eng 2023; 67: 112-122. https://doi.org/10.3311/PPci.20885

[21] Manikandan R, Ramamurthy K. Swelling characteristic of bentonite on pelletization and properties of fly ash aggregates. J Mater Civ Eng 2009; 21: 578-586. https://doi.org/10.1061/(ASCE)0899-1561(2009)21:10(578)

[22] A. Sivakumar. Pelletized fly ash lightweight aggregate concrete: A promising material. J Civ Eng Constr Technol 2012; 3: 42-48. https://doi.org/10.5897/JBD11.088

[23] Sabr HA, Abbas WA. Influence of fiber types on the properties of the artificial cold-bonded lightweight aggregates. Open Eng 2024; 14: 20220498. https://doi.org/10.1515/eng-2022-0498

[24] Yıldırım H, Özturan T. Impact resistance of concrete produced with plain and reinforced cold-bonded fly ash aggregates. J Build Eng 2021; 42: 102875. https://doi.org/10.1016/j.jobe.2021.102875

[25] Ibrahim HA, Abbas WA. Production of Cold-Bonding Pelletized Artificial Expired Cement-Fly Ash Lightweight Aggregates with Various Curing Regime. Tikrit J Eng Sci 2024; 31: 184-197. https://doi.org/10.25130/tjes.31.2.18

[26] Manikandan R, Ramamurthy K. Effect of curing method on characteristics of cold bonded fly ash aggregates. Cem Concr Compos 2008; 30: 848-853. https://doi.org/10.1016/j.cemconcomp.2008.06.006

[27] Tang P, Brouwers HJH. The durability and environmental properties of self-compacting concrete incorporating cold bonded lightweight aggregates produced from combined industrial solid wastes. Constr Build Mater 2018; 167: 271-285. https://doi.org/10.1016/j.conbuildmat.2018.02.035

[28] Tajra F, Abd Elrahman M, Chung S-Y, et al. Performance assessment of core-shell structured lightweight aggregate produced by cold bonding pelletization process. Constr Build Mater 2018; 179: 220-231. https://doi.org/10.1016/j.conbuildmat.2018.05.237

[29] Gu E, Turan O. Shrinkage cracking of lightweight concrete made with cold-bonded fly ash aggregates. 2004; 34: 1121-1130. https://doi.org/10.1016/j.cemconres.2003.11.024

[30] Joseph G, Ramamurthy K. Autogenous curing of cold-bonded fly-ash-aggregate concrete. J Mater Civ Eng 2011; 23: 393-401. https://doi.org/10.1061/(ASCE)MT.1943-5533.0000177

[31] Gesoğlu M, Özturan T, Güneyisi E. Effects of fly ash properties on characteristics of cold-bonded fly ash lightweight aggregates. Constr Build Mater 2007; 21: 1869-1878. https://doi.org/10.1016/j.conbuildmat.2006.05.038

[32] Di Mundo R, Petrella A, Notarnicola M. Surface and bulk hydrophobic cement composites by tyre rubber addition. Constr Build Mater 2018; 172: 176-184. https://doi.org/10.1016/j.conbuildmat.2018.03.233
[33] Ahmad J, Zhou Z, Majdi A, et al. Overview of Concrete Performance Made with Waste Rubber Tires: A Step toward Sustainable Concrete. Materials (Basel) 2022; 15: 5518. https://doi.org/10.3390/ma15165518
[34] Asutkar P, Shinde SB, Patel R. Study on the behaviour of rubber aggregates concrete beams using analytical approach. Eng Sci Technol an Int J 2017; 20: 151-159. https://doi.org/10.1016/j.jestch.2016.07.007
[35] Roychand R, Gravina RJ, Zhuge Y, et al. A comprehensive review on the mechanical properties of waste tire rubber concrete. Constr Build Mater 2020; 237: 117651. https://doi.org/10.1016/j.conbuildmat.2019.117651
[36] Salam N, Khalil WI. The Effect of Scrap Tires Recycled Steel Fibers on Some Hardened Properties of Green SCC. Eng Technol J 2022; 40: 810-818. https://doi.org/10.30684/etj.2022.132605.1133
[37] Motloq RF, Khalil WI, Dawood ET. Some Properties of Sustainable Concrete with Rubber Waste Aggregate. Eng Technol J 2023; 41: 1337-1345. https://doi.org/10.30684/etj.2023.140271.1458
[38] BS EN 197-1:2011. Cement - Composition, specifications and conformity criteria for common cements.
[39] Al-Jiboory YM, Al-hazaa SH. Assessment of Altawseea Ordinary Portland Cement Northern Iraq: Mineralogy, Microstructure, and Hydration. Iraqi Geol J 2022; 200-210. https://doi.org/10.46717/igj.55.2C.15ms-2022-08-28
[40] Neville AM, Brooks JJ. Concrete Technology, 2nd Editio. Edinburgh, Engl Pearson Educ Ltd.
[41] Ibrahim HA, Abbas WA. An experimental investigation of sustainable self-compacting concrete with expired cement cold bonded fly ash lightweight aggregate on strength and permeability. In: AIP Conference Proceedings. AIP Publishing, 2024. Epub ahead of print 2024. https://doi.org/10.1063/5.0237179
[42] Yu Y, Ge Y, Liu P. Recycling of expired cement and aged supplementary cementitious materials based on close packing theory and space filling effect. J Clean Prod; 239. Epub ahead of print 2019. https://doi.org/10.1016/j.jclepro.2019.118064
[43] ASTM C618. Standard Specification for Coal Fly Ash and Raw or Calcined Natural Pozzolan for Use, Annu. B. ASTM Stand., (C), (2010) 3-6. 1-3.
[44] ASTM C33/C33M-18. Standard specification for concrete aggregates. Philadelphia, PA Am Soc Test Mater. Epub ahead of print 2003.
[45] Mohesson HM, Abbas WA. Effect of Biopolymer Alginate on some properties of concrete. J Eng 2020; 26: 121-131. https://doi.org/10.31026/j.eng.2020.06.10
[46] ASTM C494/C494M-17. Standard specification for chemical admixtures for concrete. Astm C494 2005; 1-10.
[47] BS EN 934-2:2001. Admixtures for concrete, mortar and grout - Part 2: Concrete admixtures - Definitions, requirements, conformity, marking and labelling. BSI Stand Publ 2003; 3-36.
[48] Performance H, Concrete S. Sika ViscoCrete ® -5930. 2015; 4-5.
[49] Abbas ML, Abbas WA. Cold-bonded lightweight synthetic aggregate involving high reactive attapulgite at different curing conditions. Eng Technol J 2023; 41: 1-14. https://doi.org/10.30684/etj.2023.139775.1442
[50] Lin J, Mo KH, Goh Y, et al. Potential of municipal woody biomass waste ash in the production of cold-bonded lightweight aggregates. J Build Eng 2023; 63: 105392. https://doi.org/10.1016/j.jobe.2022.105392
[51] Abbas WA, Abbas ML. Physico-durability aspects of partial substitution via pelletized fly ash lightweight nano-silica concrete. Res Eng Struct Mater 2023; 9: 475-491.
[52] İpek S, Mermerdaş K. Experimental & computational study on fly ash and kaolin based synthetic lightweight aggregate. Comput Concr An Int J 2020; 26: 327-342.
[53] ASTM C330. Standard Specification for Lightweight Aggregates for Structural Concrete. ASTM Int 2009; 552: 4.
[54] BS 812-110:1990. Testing aggregates - Methods for determination of aggregate crushing value (ACV). BS 812; 110.
[55] ASTM C127-15. Standard Test Method for Density, Relative Density (Specific Gravity), and Absorption of Coarse Aggregate. ASTM Stand B 2013; 1-6.
[56] Sabr HA, Abbas WA. Study the Influence of Curing Methods on Fiber- Reinforced Cold-Bonded Artificial Lightweight Aggregate and Its Effect on Lightweight Concrete Properties. University of Technology, 2023.
[57] Reddy MVS, Nataraja MC, Sindhu K. Performance of Light Weight Concrete using Fly Ash Pellets as Coarse Aggregate Replacement. 2016; 9: 95-104.
[58] González-Corrochano B, Alonso-Azcárate J, Rodas M, et al. Microstructure and mineralogy of lightweight aggregates manufactured from mining and industrial wastes. Constr Build Mater 2011; 25: 3591-3602. https://doi.org/10.1016/j.conbuildmat.2011.03.053

[59] Bai Y, Ibrahim R, Basheer PAM. Properties of lightweight concrete manufactured with fly ash, furnace bottom ash, and lytag. In: International workshop on sustainable development and concrete technology. Center for Transportation Research and Education, Iowa State University, 2004, pp. 77-88.
[60] Güneyisi E, Gesoğlu M, Booya E. Fresh properties of self-compacting cold bonded fly ash lightweight aggregate concrete with different mineral admixtures. Mater Struct 2012; 45: 1849-1859. https://doi.org/10.1617/s11527-012-9874-6
[61] ACI 211.2-98. Standard Practice for Selecting Proportions for Structural Lightweight Concrete. Am Concr Inst 1998; 1-18.
[62] BS EN 12390-3:2019. Testing hardened concrete-Part 3: Compressive strength of test specimens. BSI Stand Publ.
[63] ASTM C597-22. Standard test method for pulse velocity through concrete. ASTM Stand C597-16, ASTM Int West Conshohocken. Epub ahead of print 2016.
[64] ASTM C642-21. Standard test method for density, absorption, and voids in hardened concrete. ASTM, ASTM Int. Epub ahead of print 2013.
[65] ASTM C496-96. Test Method for Splitting Tensile Strength of Cylindrical Concrete Specimens. ASTM International 1996; 1: 5-7.
[66] ASTM C78/C78M-21. Standard Test Method for Flexural Strength of Concrete (Using Simple Beam with Third-Point Loading). ASTM Int 2010; 1: 5-7.
[67] ASTM C469. Standard Test Method for Static Modulus of Elasticity and Poisson's Ratio of Concrete in Compression. ASTM Stand 2014; 04: 1-5.
[68] Ibrahim HA, Abbas WA. Synergistic Effects of Composite Expired Cement Fly Ash Cold-bonding Aggregates and Mineral Admixtures on Mechanical and Drying Shrinkage Performance of Sustainable Self-compacted Concrete. Int J Eng 2024; 37: 2276-2287. https://doi.org/10.5829/IJE.2024.37.11B.13
[69] Ibrahim H, Abbas W. Behavior of Self-Compacted Lightweight Concrete Containing Cold Bonded Aggregate. University of Technology, 2024.
[70] Mehta PK, Monteiro P. Concrete: microstructure, properties, and materials. Epub ahead of print 2006.
[71] Bui LA, Hwang C, Chen C, et al. Manufacture and performance of cold bonded lightweight aggregate using alkaline activators for high performance concrete. Constr Build Mater 2012; 35: 1056-1062. https://doi.org/10.1016/j.conbuildmat.2012.04.032
[72] Wu W, Wang R, Zhu C, et al. The effect of fly ash and silica fume on mechanical properties and durability of coral aggregate concrete. Constr Build Mater 2018; 185: 69-78. https://doi.org/10.1016/j.conbuildmat.2018.06.097
[73] ASTM C 597-02. Standard test Method For Pulse Velocity Through Concrete. United States Am Soc Test Mater 2003; 04: 3-6.
[74] Güneyisi E, Gesoglu M, Azez OA, et al. Physico-mechanical properties of self-compacting concrete containing treated cold-bonded fly ash lightweight aggregates and SiO2 nano-particles. Constr Build Mater 2015; 101: 1142-1153. https://doi.org/10.1016/j.conbuildmat.2015.10.117
[75] ACI. 318-19 Building Code Requirements for Structural Concrete and Commentary. 2019. Epub ahead of print 2019.
[76] Lakhiar MT, Kong SY, Bai Y, et al. Thermal and mechanical properties of concrete incorporating silica fume and waste rubber powder. Polymers (Basel) 2022; 14: 4858. https://doi.org/10.3390/polym14224858
[77] Tajra F, Abd Elrahman M, Stephan D. An experimental study of using core-shell structured lightweight aggregate in producing lightweight concrete. In: International Conference on Sustainable, Environmental Friendly Construction Materials, ICSEFCM. 2018, pp. 35-40.
[78] Samadar Salim. Fracture and Permeability Properties of Artificial Fly Ash and Slag aggregate Concretes at Different Water-to-Cement Ratios. J Mater Sci Technol Res 2020; 7: 11-29. https://doi.org/10.31875/2410-4701.2020.07.02
[79] Atmaca N, Abbas ML, Atmaca A. Effects of nano-silica on the gas permeability, durability and mechanical properties of high-strength lightweight concrete. Constr Build Mater 2017; 147: 17-26. https://doi.org/10.1016/j.conbuildmat.2017.04.156
[80] Mermerdaş K, İpek S, Algın Z, et al. Combined effects of microsilica, steel fibre and artificial lightweight aggregate on the shrinkage and mechanical performance of high strength cementitious composite. Constr Build Mater 2020; 262: 120048. https://doi.org/10.1016/j.conbuildmat.2020.120048
[81] Hatami F, Amiri M. Experimental study of mechanical properties and durability of green concrete containing slag, waste rubber powder and recycled aggregate with artificial neural network. Clean Mater 2022; 5: 100112. https://doi.org/10.1016/j.clema.2022.100112
[82] ACI 213 R. Guide for Structural Lightweight-Aggregate Concrete. Concrete 2014; 0-39.
[83] Salim S. Fracture and permeability properties of artificial fly ash and slag aggregate concretes at different water-to-cement ratios. J Mater Sci Technol Res 2020; 7: 11-29. https://doi.org/10.31875/2410-4701.2020.07.02

[84] Tajra F, Abd Elrahman M, Stephan D. The production and properties of cold-bonded aggregate and its applications in concrete: A review. Constr Build Mater 2019; 225: 29-43. https://doi.org/10.1016/j.conbuildmat.2019.07.219

[85] Wu B, Ye G. Development of porosity of cement paste blended with supplementary cementitious materials after carbonation. Constr Build Mater 2017; 145: 52-61. https://doi.org/10.1016/j.conbuildmat.2017.03.176